CHALMERS
UNIVERSITY OF TECHNOLOGY

Unequal bit error probability in coherent QPSK fiber-optic systems using phase modulator based transmitters

Unequal Bit Error Probability in Coherent QPSK Fiber Optic Systems Using Phase Modulator Based Transmitters

Hongxia Zhao[†], Erik Agrell[†], Magnus Karlsson[‡]

[†]Department of Signals and Systems, Chalmers University of Technology, 412 96 Göteborg, Sweden. Email: hz,agrell@chalmers.se

[‡]Department of Microtechnology and Nanoscience, Chalmers University of Technology, 412 96 Göteborg, Sweden.

***Abstract*— We report on the occurrence of unequal bit error probability in a coherent quadrature phase shift keying (QPSK) fiber optic system. The bit error rates (BER) of two QPSK bits are derived individually based on the developed system model, and they turn out to differ by more than an order of magnitude for a phase modulator based transmitter. The phenomenon, previously unreported, arises because such a transmitter introduces a controlled form of inter-symbol-interference (ISI), and the receiver low-pass filters affect this ISI differently for the two bits. The optimum bandwidth of the receiver low-pass filter is obtained from the analytic derivation, which is about 0.7 times the symbol rate. We propose two simple system modifications, one in the transmitter and one in the receiver, to compensate for the phenomenon and equalize the two BER's. Those modifications improve the system performance by about 2 dB without adding any extra hardware.**

I. Introduction

Since the first fiber optical communication system was launched in 1977, the transmission bit rate has increased from Mb/s to Tb/s today [1]. Most currently deployed fiber communication systems are still using on-off keying (OOK), although a few are starting to use differential phase-shift keying (DPSK). Both OOK and DPSK have spectral efficiencies of 1 b/s/Hz, which limits the potential transmission capacity in future optical networks. Therefore, non-binary modulation formats with high spectral efficiency have recently received renewed interest in fiber optic communications. Among the multilevel modulation formats that can achieve 2 b/s/Hz, quadrature phase-shift keying (QPSK) with differentially coherent detection or coherent detection is very promising in wavelength-division multiplexed (WDM) systems, due to the reasonable complexity and superior transmission characteristics, such as higher tolerance to fiber chromatic dispersion and polarization-mode dispersion [2]–[7]. Coherent detection offers better sensitivity and yields a better performance, however, at the cost of a more complex implementation compared to differential detection [3].

The well established analytical models for digital wireless communications (see for instance [8]) are not directly applicable to fiber optic communications, where the transmitted signal is generated differently and the optical receiver is imperfect. Previous works on performance evaluation of fiber optic systems were either based on OOK modulation without optical preamplification [9], [10], or with optical preamplification but using amplitude shift keying (ASK), frequency shift keying (FSK) and DPSK modulation [11]. Early works on coherent QPSK optical systems rarely considered transmitter structures [12]–[15], while a few recent papers have started to discuss the impact of the transmitter and present results from simulations or experiments [7], [16], [17]. To the best of the authors' knowledge, there is only one paper that has discussed individual performances of two QPSK bits in a coherent optical system [15], where the QPSK signal is naturally mapped, which undoubtably gives rise to different bit performances.

In this paper, we present and analyze a coherent fiber optic system using QPSK modulation and optical preamplification. The joint impact of non-ideal transmitters and receivers is here studied for the first time. While analyzing this system, we have found that the two bits in a Gray mapped QPSK symbol have unequal bit error rates (BER), which has never been reported before. Based on our system model, we can explain the unequal BER phenomenon and derive the theoretical system performance. In addition, the optimum low-pass (LP) filter bandwidth is computed, which is about 0.7 times the transmission symbol rate. This result supports a commonly used LP filter bandwidth design rule, e.g., the LP filter bandwidth in experiments and simulations of fiber optic systems is often chosen to be 0.6 to 0.8 times the transmission rate [18]–[20]. Furthermore, according to our theoretical analysis, two simple system modifications are proposed to improve the whole system

performance by just adjusting coefficients of the mapping unit at the transmitter or decision boundaries at the receiver.

The rest of the paper is organized as follows: In Section II, a realistic coherent QPSK fiber optic system model is developed. Section III presents the simulated BER results as well as the explanation of the unequal bit error probability. The theoretical BER calculations are derived in Section IV. Section V presents the optimum bandwidth of the receiver low-pass filter. In Section VI, we propose two system modifications and show the system performance improvement. Finally, some discussion and conclusions are summarized in Section VII.

II. System Model

A coherent QPSK fiber optic system with a symbol rate of 10 Gsymbols/s is studied. Due to the attractive spectral efficiency, the coherent QPSK transmission is a strong candidate for use over a single-wavelength channel in future WDM systems. Since this study will focus on the transmitter and receiver properties, we assume that an ideal fiber is used, and the discussion of fiber dispersion and nonlinearity effects will not be included in this paper. Such a system is a so called back-to-back system in fiber communications.

In a long-haul fiber optic systems, the optical amplified spontaneous emission noise is the dominant noise source; we therefore ignore the thermal and shot noise in our study. The pulse format used in the system is the nonreturn-to-zero (NRZ) format. A return-to-zero (RZ) format can be utilized by applying a pulse carver to the NRZ pulses. Since the RZ pulse has a narrower pulse width, it is less sensitive to inter-symbol interference (ISI) compared to an NRZ pulse, thus the quality of the eye diagram is improved and a better performance can be achieved [21]–[23]. However, RZ formats increase the complexity of the system. Other drawbacks of the RZ format are that it requires a higher peak power and consumes more bandwidth as shown in [22]. When using OOK, the NRZ format is commonly used in high data rate WDM systems because of the robustness to fiber dispersion compared to the RZ format [24], [25].

A. Transmitter

The optical transmitter is based on an ideal continuous wave (CW) laser and an external modulation. There exist different QPSK transmitters with varying complexity. In [16], three phase modulator based transmitters are discussed in a differential QPSK (DQPSK) context. We show the two simplest transmitters in Fig. 1. In the following, these two transmitters are referred to as TX-A and TX-B, respectively. TX-A uses two modulators that are connected serially, while TX-B uses a single modulator. Note that the single modulator in TX-B can be a dual-drive Mach-Zehnder modulator or a phase modulator. In this paper, a phase modulator is used, which in fact is equivalent to one of the cases of generating QPSK signals with a dual-drive Mach-Zehnder modulator in [21], [26].

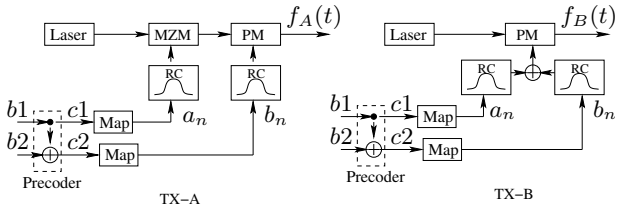

Fig. 1. QPSK transmitter A (TX-A) and transmitter B (TX-B).

In principle, the transmitters convert the CW light radiated from the laser into a data-coded pulse train with the proper modulation format. Since the transmitted bits modulated by the standard modulators used in fiber optic systems are naturally mapped, a simple precoder (dashed area in the figure) is applied to realize a Gray mapping for the transmitted information bits, bit 1, $b1$, and bit 2, $b2$. The algorithm of this precoder is $c1 = b1$ and $c2 = b1 \oplus b2$, where $c1$ and $c2$ are the coded bits. Thus, naturally mapped information bits result in Gray mapped coded bits, or vice versa. The coded bits then map to a_n and b_n such that $a_n \in \{-1, 1\}$ and $b_n \in \{0, 1\}$. To model the limited temporal response of the transmitter, we use a raised cosine (RC) impulse shaper, which has the time-domain impulse response [16]

$$p(t) = \begin{cases} 1, & |t| \le \frac{T}{2}(1-\alpha) \\ \cos^2\left[\frac{\pi}{4}\frac{2|t|-T(1-\alpha)}{\alpha T}\right], & \frac{T}{2}(1-\alpha) \le |t| \le \frac{T}{2}(1+\alpha) \\ 0, & |t| > \frac{T}{2}(1+\alpha) \end{cases}$$

where T is the symbol duration and α is the roll-off factor. To get better power efficiency, the roll-off factor is normally chosen to be non-zero such that the adjacent NRZ pulses overlap each other and the envelop of the transmitted signal is constant if same symbols are transmitted, which in turn results inter-symbol interference in the transmitted signal.

MZM and PM in the figure stand for Mach-Zehnder modulator, which is an amplitude modulator, and $\pi/2$ phase modulator, respectively. From the transfer functions of MZM and PM [27], the baseband equivalent transmitted signals of TX-A and TX-B, denoted as $f_A(t)$

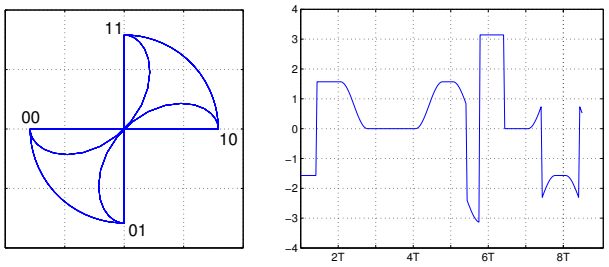

Fig. 2. Left: signal constellation of $f_A(t)$. Right: phase of $f_A(t)$ for the bit sequence (01,11,10,10,11,00,10,01).

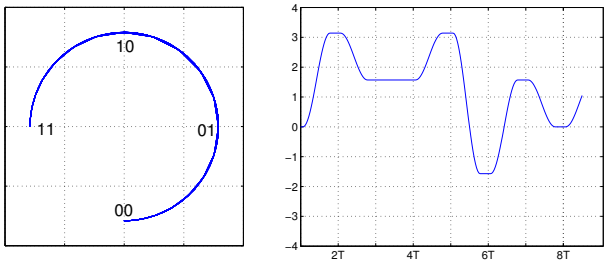

Fig. 3. Left: signal constellation of $f_B(t)$. Right: phase of $f_B(t)$ for the bit sequence (01,11,10,10,11,00,10,01).

and $f_B(t)$, respectively, are

$$f_A(t) = \sin\left[\frac{\pi}{2}\sum_n (a_n p(t-nT))\right] e^{j\frac{\pi}{2}\sum_n b_n p(t-nT)}, \tag{1}$$

and

$$f_B(t) = e^{j\frac{\pi}{2}\sum_n (a_n+b_n)p(t-nT)}. \tag{2}$$

Both modulators would produce the same output signal if a rectangular pulse $p(t)$ is used. However, with any smooth pulse such as the RC pulse, the transitions between phases are different, as shown in Figs. 2 and 3. The different transition patterns result in different signal constellations at the output of the receiver, which in turn gives different BER's, as we will see in the next section.

In Fig. 2 and 3, we show the signal constellation and phase of $f_A(t)$ and $f_B(t)$. The signal constellation is the instantaneous amplitude and phase of the transmitted signal. The bits of QPSK symbols, $\{00, 01, 10, 11\}$, shown in the figures represent the coded bits $\{c1c2\}$, which is different from the following signal constellation figures in which we show the information bits $\{b1b2\}$.

B. Receiver

Coherent detection in fiber optic systems becomes feasible with the help of high speed digital signal processing (DSP). In this paper, a coherent receiver discussed in e.g. [13], [28] is used. The DSP-based

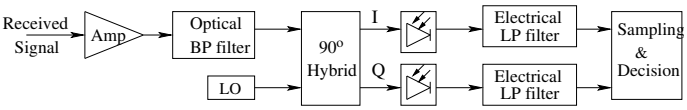

Fig. 4. Structure of the optical coherent QPSK receiver.

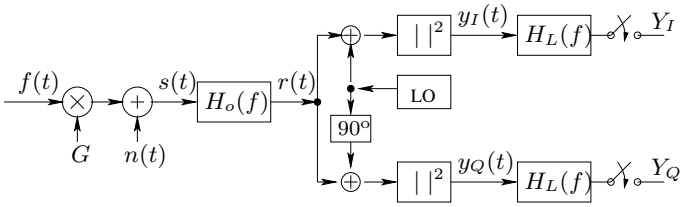

Fig. 5. Equivalent baseband receiver model.

detection scheme in [28] estimates the carrier phase with respect to an auxiliary laser with the same wavelength as the received signal but unknown phase. The net result, after compensating for the phase offset in a DSP, is the same as if a phase-locked local oscillator (LO) was used, which is therefore assumed in the following model, where the baseband LO signal is written as a real signal with constant power.

The structure of the receiver is shown in Fig. 4. At the front of the receiver, the received signal is first amplified by an Erbium-Doped Fiber Amplifier (EDFA) (Amp in the figure), then the amplified signal is passed through an optical bandpass (BP) filter. The 90^o Hybrid combines the output of the BP filter with a LO light wave and splits the combined signal in in-phase (I) and quadrature (Q) branches. In each branch, a photo diode followed by an electrical low-pass filter is used. We assume that the output of the photo diode is DC-free, which can easily be realized in practice by using a filter. Finally, a sampling and decision unit makes a decision based on the output of the two branches.

The above coherent receiver can be modelled as shown in Fig. 5, where G, $n(t)$, $H_o(f)$ and $H_L(f)$ represent the gain of EDFA, the optical noise, and the frequency response (low-pass equivalent) of the BP and LP filters, respectively. The decision made from the output of I and Q branches, Y_I and Y_Q, define the received bits of the QPSK symbol, which should, in the absence of transmission errors, recover $b1$ and $b2$, respectively. In this paper, we assume a unit responsivity of the photo diodes so that they provide squared-law operations[1].

The optical noise $n(t)$ is commonly modelled as a zero-mean additive white Gaussian noise (AWGN) with single-sided noise power spectral density $N_0 = \frac{F}{2}h\nu G$,

[1]The assumption is just for notation simplicity and will not affect the conclusions.

where F is the amplifier noise figure, $h\nu$ is the photon energy, and G is the optical amplifier gain, respectively. Although the optimum bandwidth of the optical BP filter is around 2–3 times the data rate depending on the modulation format, the transmitter characteristic etc [18], [29], a sufficiently stable narrow-band optical filter is not a realistic solution, the BP filter in this paper is chosen to have a 3 dB bandwidth of 40 GHz and have a Gaussian frequency response. The equivalent baseband frequency response of the BP filter is

$$H_o(f) = e^{\frac{2\ln 2 \cdot f^2}{B^2}}, \tag{3}$$

where B is the bandwidth.

The design of the low-pass filters, which are realized on the electrical side of the receiver, offers more flexibility than the bandpass filter. Because of the ISI existing in the transmitted signal due to the nonzero roll-off factor of the pulse shaper, and the nonlinear characteristics of the photo diodes, a full optimization of the filter responses is a formidable problem in itself [30] and beyond the scope of this paper. Under the condition of only optimizing the cutoff frequency, we choose the LP filters as Butterworth filters, which are commercially available and commonly used in fiber optic systems (see e.g. [31] and references therein). The frequency response of a Butterworth filter is

$$H_L(f) = \sqrt{\frac{1}{1 + (f/f_c)^{2N}}}, \tag{4}$$

where N is the order of the filter and f_c is the cutoff frequency.

III. Simulated BER results

In all the simulations, random independent information bits with a total bit rate of 20 Gb/s are used. The roll-off factor α of the RC pulse $p(t)$ is set to be 0.7 in the simulations. The BER was estimated after 50–100 bit errors had occurred.

At the receiver, the gain and noise figure of the EDFA amplifier are set to be 30 dB and 5 dB, respectively. The carrier wavelength is equal to 1550 nm and the bandwidth of the BP filter is 40 GHz. The Butterworth LP filters have an order of $N = 3$ in all simulations.

When using transmitter TX-A and TX-B, the simulated BER performance versus E_b/N_0 are plotted in Figs. 6 and 7, respectively. The E_b/N_0 is the ratio between bit energy and single-sided noise spectral density before the optical BP filter. The Butterworth LP filter has a cutoff frequency of $f_c = 7$ GHz. Because TX-B has a simpler structure than TX-A, it is not a surprise to see that the system using TX-A performs better than the system using TX-B, which has also been reported

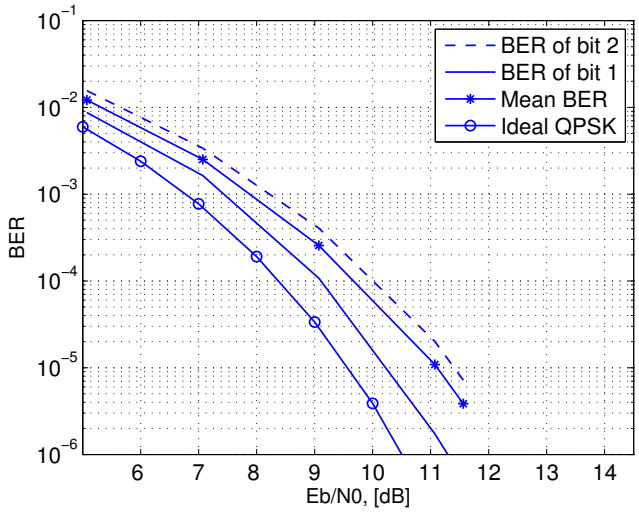

Fig. 6. Unequal BER of two QPSK bits when using TX-A.

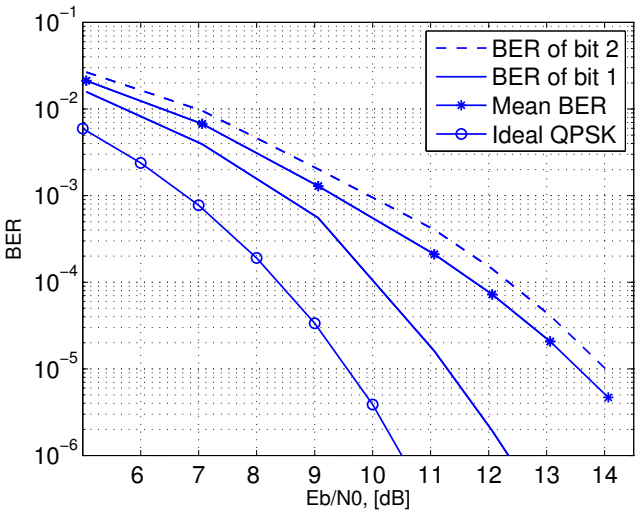

Fig. 7. Unequal BER of two QPSK bits when using TX-B.

for differential QPSK systems in [16]. For comparison, the performance of an ideal QPSK system is included in the diagrams, under the assumptions of white Gaussian noise, no ISI, and maximum likelihood detection.

The unequal bit error probability can be easily observed in the figures. For example, at an E_b/N_0 of 11 dB, bit 1 of the QPSK symbol performs ten times (when using TX-A) and more than ten times (when using TX-B) better than bit 2.

In Fig. 8, when the systems are noise free, the signal constellation after sampling the LP filter output are plotted, which explains the unequal BER phenomenon. The signal constellation is asymmetric, which is due to the transition patterns between constellation points (see Figs. 2 and 3), the ISI introduced by the transmitter, and the receiver filtering. This asymmetric signal constellation gives rise to the different performances of QPSK

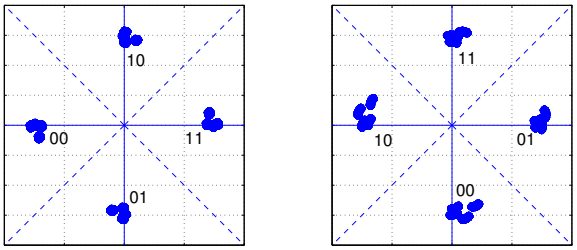

Fig. 8. Simulated signal constellation of the sampled LP filter output when using TX-A (left) and TX-B (right) at $E_b/N_0 = 11$ dB, $f_c = 7$ GHz.

bits. As seen in the figure, the signal constellation of a system using TX-B is more spread and dislocated than that of a system using TX-A. In particular, the points move closer to the decision boundary corresponding to $b2$ than the one corresponding to $b1$. This occurs for both transmitters, but most noticeable for TX-B, which explains why the BER difference is larger for the system using TX-B. In fact, the ISI is strongly related to the cutoff frequency of the LP filters as we will present in the next two sections, where a large cutoff frequency gives a more symmetric signal constellation and results in less performance difference between the two bits.

IV. Theoretical BER results

In this section, based on the system model described above, the theoretical bit error rate of a QPSK fiber optic system with coherent detection is derived. We assume that the ISI only occurs between two consecutive symbols even after the receiver filters. Although this assumption is accurate only above a certain LP filter cutoff frequency, systems with a smaller cutoff frequency have an inferior performance and are therefore less interesting.

For a back-to-back system, the received signal is the same as the transmitted signal. Thus, at the front of the receiver, the received signal $f(t)$ in Fig. 5 equals either $f_A(t)$ (when using TX-A) or $f_B(t)$ (when using TX-B). The amplified signal $s(t)$ can be written as $s(t) = Gf(t)+n(t)$. Since the bandwidth of the received signal $f(t)$ is much smaller than the BP filter bandwidth, we can write the signal after the BP filter as $r(t) = Gf(t)+\hat{n}(t)$, where $\hat{n}(t)$ is the noise $n(t)$ filtered by the BP filter $H_o(f)$. It can be shown that $\hat{n}(t)$ has zero mean and is Gaussian distributed due to the fact that $n(t)$ is zero-mean white Gaussian noise and the BP filter is linear [8, sec. 2.2.3].

In complex notation, the baseband signal $r(t)$ can be written as $r(t) = A_s(t)e^{-j\phi(t)} + N_s(t)e^{-j\theta(t)}$, where A_s, N_s, $\phi(t)$, and $\theta(t)$ are the amplitude and phase of the desired signal and the noise, respectively. With this notation and the assumption of a real LO signal with constant amplitude $\sqrt{P_{LO}}$, the signals after the photo diodes at the I and Q branches are

$$\begin{aligned} y_I(t) &= \left|r(t) + \sqrt{P_{LO}}\right|^2 \\ &= 2\sqrt{P_{LO}}\,\mathrm{Re}\{r(t)\} + N_s^2(t) \\ &\quad + 2A_s(t)N_s(t)\cos(\phi(t)-\theta(t)) + A_s^2(t) + P_{LO}, \end{aligned} \tag{5}$$

$$\begin{aligned} y_Q(t) &= \left|r(t) + j\sqrt{P_{LO}}\right|^2 \\ &= 2\sqrt{P_{LO}}\,\mathrm{Im}\{r(t)\} + N_s^2(t) \\ &\quad + 2A_s(t)N_s(t)\cos(\phi(t)-\theta(t)) + A_s^2(t) + P_{LO}. \end{aligned} \tag{6}$$

It is reasonable to assume that the power of LO signal, P_{LO}, is much larger than that of the BP output signal $r(t)$, which means that the optical noise from the first term of equation (5) and (6), $2\sqrt{P_{LO}}\,\mathrm{Re}\{r(t)\}$ and $2\sqrt{P_{LO}}\,\mathrm{Im}\{r(t)\}$, are the dominant noise sources. The other noise contributions, terms 2 and 3 of the equations, $N_s^2(t) + 2A_s(t)N_s(t)\cos(\phi(t)-\theta(t))$, are negligible. Terms 4 and 5 of the equations are the DC components[2], which are removed from the signal filtering, see Sec. II-B. As shown in Fig. 9, the noise histogram of (5) with all noise contributions, i.e., the first three terms of the equation, is almost the same as only considering the noise from the first term. Thus, we can simplify (5) and (6) as $y_I(t) = 2\sqrt{P_{LO}}\,\mathrm{Re}\{r(t)\}$ and $y_Q(t) = 2\sqrt{P_{LO}}\,\mathrm{Im}\{r(t)\}$.

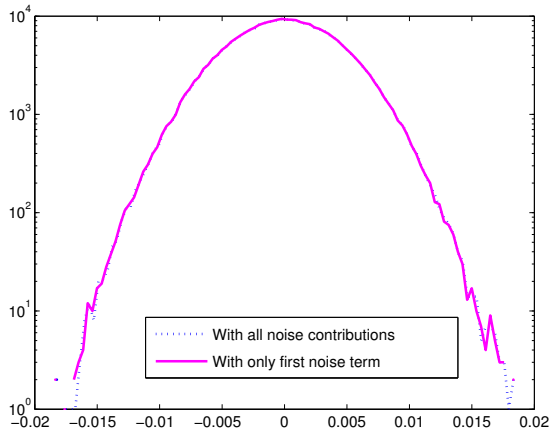

Fig. 9. Noise histogram of equation (5). Dashed line: Using the first three terms of the equation. Solid line: Using only the first term of the equation.

[2]Term 4 of the equations, $A_s^2(t)$, is varying slowly compared with the optical noise and is therefore treated as a DC component.

To calculate the BER, the LP filter outputs are separated into two parts, the desired signal part and the noise part, which is written as $Y_I = S_I + N_I$ and $Y_Q = S_Q + N_Q$. Since the simplified LP filter input signals are proportional to the real and imaginary parts of $r(t)$, respectively, the real and imaginary parts of complex noise $n(t)$ contribute to the LP filter output noises N_I and N_Q, respectively. Hence, N_I and N_Q are independent and Gaussian, with zero mean and variance [8]

$$\sigma^2 = 4P_{LO} \cdot \frac{N_0}{2} \int_{-\infty}^{\infty} |H_o(f)|^2 \, |H_L(f)|^2 \, df \qquad (7)$$

The desired signal part of the LP filter outputs, S_I and S_Q, are the convolution of the LP filter impulse response with the signal components of the simplified $y_I(t)$ and $y_Q(t)$, respectively. For the Butterworth filter of order 3 with the frequency response given by (4), the impulse response is

$$\begin{aligned} h_L(t) =& 2\pi f_c \Big(e^{-2\pi f_c t} - e^{-\frac{2\pi f_c t}{2}} \cos(0.866 \cdot 2\pi f_c t) \\ &+ 0.5774 e^{-\frac{2\pi f_c t}{2}} \sin(0.866 \cdot 2\pi f_c t) \Big). \end{aligned}$$

Assuming that the LP filter only affects two consecutive symbols, which is a reasonably accurate approximation for high filter bandwidth, see Sec. V, the desired signals can be written as

$$S_I = \int_{\rho T}^{(2+\rho)T} 2\,\mathrm{Re}\{Gf(\tau)\} \cdot h_L(2T - \tau) d\tau, \qquad (8)$$

$$S_Q = \int_{\beta T}^{(2+\beta)T} 2\,\mathrm{Im}\{Gf(\tau)\} \cdot h_L(2T - \tau) d\tau. \qquad (9)$$

where $0 \le \rho \le 0.7$, $0 \le \beta \le 0.7$, and their values are chosen by numerically optimizing the BER performance.

In Fig. 10, we plot the analytic signal constellation of the LP filter output, in which S_I and S_Q generate 16 symbols in a two-dimensional plane[3]. The dashed lines in the figures are the decision boundaries, which are the same as in the simulations. The distances, $d_{12}, d_{21}, \cdots, d_{14}$, shown in the figure are the orthogonal distances from each symbol point to the boundary, i.e., there are four different d_{12} and so on.

Given the distances and the noise variance, the BER of QPSK symbol bit 1 and bit 2, P_1 and P_2, can be calculated as

[3]Because ISI is assumed to occur only within two consecutive symbols, this simplified model considers only 16 received QPSK symbols.

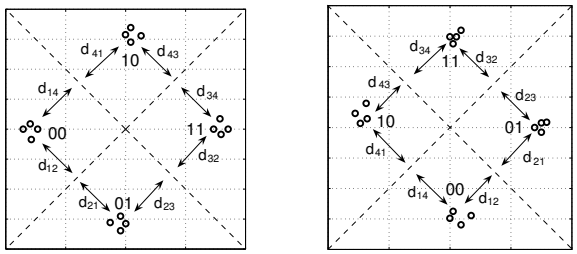

Fig. 10. Analytical signal constellation when using TX-A (left) and TX-B (right), $E_b/N_0 = 11$ dB, $f_c = 7$ GHz.

$$\begin{aligned} P_1 =& \frac{1}{16} \sum_{i=1}^{4} \Big[Q\left(\frac{d_{23}(i)}{\sigma}\right) + Q\left(\frac{d_{32}(i)}{\sigma}\right) \\ &+ Q\left(\frac{d_{14}(i)}{\sigma}\right) + Q\left(\frac{d_{41}(i)}{\sigma}\right) \Big], \end{aligned} \qquad (10)$$

$$\begin{aligned} P_2 =& \frac{1}{16} \sum_{i=1}^{4} \Big[Q\left(\frac{d_{12}(i)}{\sigma}\right) + Q\left(\frac{d_{21}(i)}{\sigma}\right) \\ &+ Q\left(\frac{d_{34}(i)}{\sigma}\right) + Q\left(\frac{d_{43}(i)}{\sigma}\right) \Big]. \end{aligned} \qquad (11)$$

where $Q(x) = \frac{1}{\sqrt{2\pi}} \int_x^{\infty} e^{-t^2/2} dt$. These expressions will be evaluated in the next section.

V. Optimum LP filter bandwidth

The bandwidth of the LP filter in fiber optic communications is often chosen to be 0.6R to 0.8R, where R is the transmission rate (see [18], [20] and references therein). In this section, the optimum LP filter bandwidth for a NRZ coherent QPSK fiber optic system is estimated analytically and by simulations, which can be compared with the bandwidth given by the commonly used rule.

In Figs. 11 and 12, the BER performance of the two QPSK bits are plotted versus the LP filter cutoff frequency, where the the signal-to-noise ratio (SNR) is fixed at $E_b/N_0 = 11$ dB. We see that on the whole, the rule-of-thumb of defining LP filter bandwidth is reasonable, but somewhat lower BER's can be achieved by modifying the bandwidth based on the precise system setup. The optimum bandwidth for TX-A is 5–6 GHz. For TX-B, it would be advantageous to use different filter bandwidths for the two bits, about 6–7 GHz for bit 1 and 8–9 GHz for bit 2, which is, however, rarely done in practice.

In Fig. 13, we plot the simulated signal constellations at cutoff frequencies of 5 GHz and 13 GHz when TX-B is used. Both simulations have the same SNR. When the cutoff frequency f_c is small, the symbol clouds are more spread and dislocated than for a large f_c, which implies

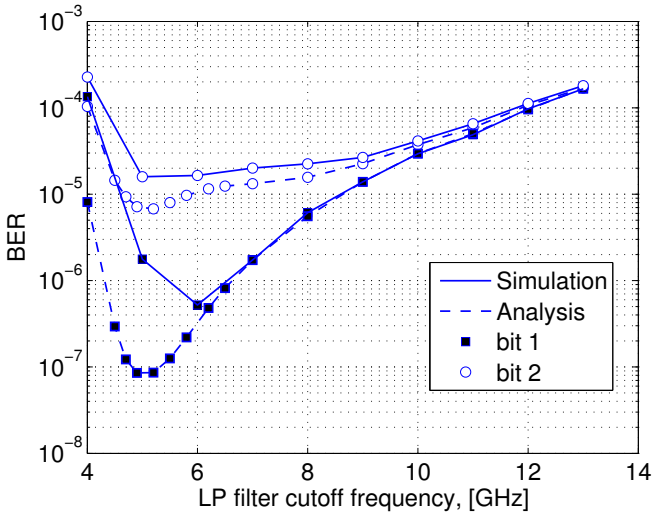

Fig. 11. Comparison of analytical BER performance with simulation results when using TX-A, $E_b/N_0 = 11$ dB.

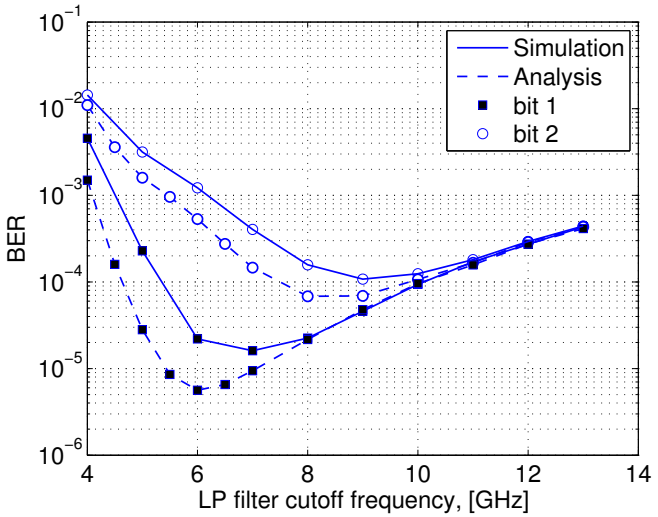

Fig. 12. Comparison of analytical BER performance with simulation results when using TX-B, $E_b/N_0 = 11$ dB.

that the assumption of 2-symbol ISI is more accurate for larger f_c. The same effect is illustrated by the LP filter impulse responses in Fig. 14. The gap between the analytic and simulation results in Figs. 11 and 12 can be reduced by involving more symbols in the ISI. However, the complexity grows exponentially with the number of symbols and the observed optimum LP filter bandwidths will not be substantially changed.

VI. System Modifications and Results

Due to the unequal BER performance, the overall system performance, i.e., the mean BER, is dominated by the worst bit performance, especially for a system using TX-B (see Fig. 7). Since transmitter TX-B has the simplest structure and is very easy to implement in

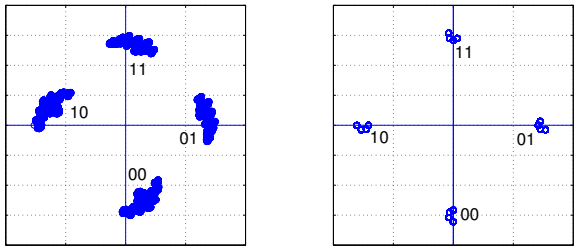

Fig. 13. Simulated signal constellation at cutoff frequencies of 5 GHz (left) and 13 GHz (right) when using TX-B, $E_b/N_0 = 11$ dB.

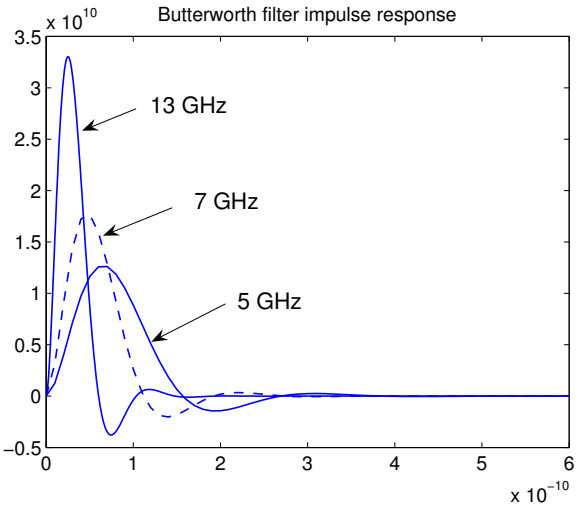

Fig. 14. LP filter impulse response at a transmitted symbol rate of 10 Gsymbols/s. The 2-symbol ISI assumption is almost true for an f_c of 13 GHz, but when f_c is 5 GHz, more symbols are involved in the ISI.

practice, although there exists a power penalty compare to other transmitters, it is still a very attractive transmitter alternative. In this section, we will focus on improving the overall system performance when transmitter TX-B is used. Two simple system modifications based on the system analysis in Sec. IV are proposed. The modifications do not need to add any new hardware, but rather require merely the adjustment of either the coefficients of the mapping unit at the transmitter or the decision boundaries at the receiver, though they still lead to significant improvements of the system performance.

A. Transmitter Modification

The transmitter is modified with the aim of minimizing the difference of the BER performance of the two QPSK bits. This will improve the overall system performance, because the average BER is dominated by the worst bit. Since the unequal BER is due to the asymmetrical signal constellation shown in Fig. 8, minimizing the performance difference becomes the same as making the signal constellation more symmetric. This approach is

TABLE I

COEFFICIENTS OF TX-B MAPPING UNIT, $E_b/N_0 = 11$ dB.

f_c [GHz]	λ	μ
4	1.145	1.09
5	1.145	1.07
6	1.11	1.055
7	1.065	1.055
8	1.035	1.03
9	1.01	1.01
10	1.005	1.005

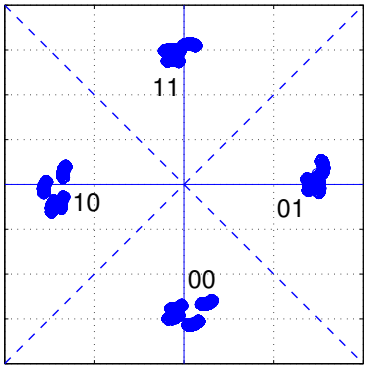

Fig. 15. Signal constellation with a modified transmitter at $f_c = 7$ GHz, $E_b/N_0 = 11$ dB.

often implemented experimentally in system fine tuning (see e.g. [14] for measured optimized and unoptimized constellations) but here we will for the first time quantify the improvement theoretically.

In Sec. IV, we have shown that the theoretical BER of bit 1 and bit 2, P_1 and P_2, are decided by the distances $d_{12}, d_{21}, \cdots, d_{14}$, which in turn are decided by the LP outputs S_I and S_Q given by (8) and (9). For a given LP filter, S_I and S_Q are affected by the received signal $f(t)$, which in a back-to-back system is the same as the transmitted signal. We therefore modify $f_B(t)$ in (2) as

$$f_B(t) = e^{j\frac{\pi}{2}\sum_n(\lambda a_n + \mu b_n)p(t-nT)}. \qquad (12)$$

and find the two coefficients λ and μ from the BER analysis in Sec. IV by numerically minimizing $(P_1 + P_2)/2$. In Table I, the optimum coefficients λ and μ are listed for different cutoff frequencies f_c.

Fig. 15 shows the simulated signal constellation when the system uses the modified transmitter. It is obvious that the symbol clouds are more symmetrically located than the original ones in Fig. 8.

The simulation results of BER versus f_c for the systems with modified transmitter TX-B are shown in Fig. 16. Clearly, the performance difference of the two QPSK bits becomes smaller. When fixing the cutoff

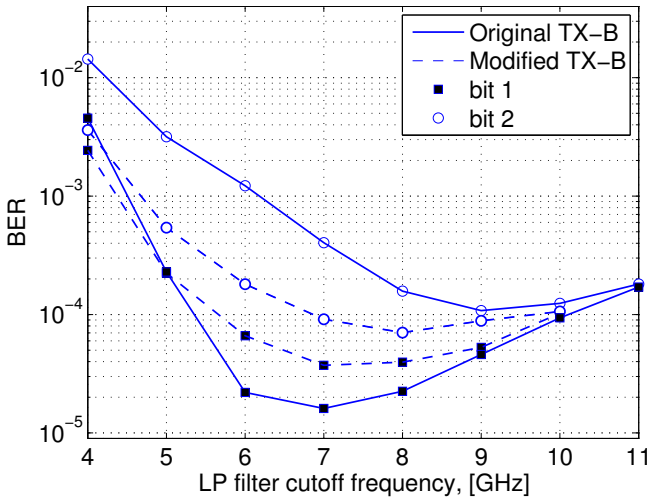

Fig. 16. Performance comparison for systems with and without modified transmitter TX-B, $E_b/N_0 = 11$ dB.

TABLE II

NEW BOUNDARY ANGLES IN FOUR QUADRANTS WHEN USING TX-B, $E_b/N_0 = 11$ dB.

f_c [GHz]	boundary angles in 4 quadrants			
4	40.3°	120.0°	−132.6°	−35.7°
5	41.5°	120.0°	−134.3°	−36.9°
6	42.6°	122.3°	−135.5°	−38.0°
7	43.8°	127.4°	−135.5°	−40.9°
8	44.3°	130.9°	−135.5°	−43.2°
9	44.9°	133.2°	−134.9°	−44.3°
10	44.9°	134.9°	−134.9°	−44.9°
11	44.9°	135.5°	−134.9°	−44.9°
12	44.9°	136.0°	−134.9°	−44.9°
13	44.9°	136.0°	−134.9°	−44.9°

frequency at 7 GHz, the mean BER performance of the system with transmitter modification is compared with the old system at the end of this section in Fig. 19. It shows that when targeting at a mean BER of 10^{-5}, more than 1 dB gain is achieved. We believe that this gain will be more than 2 dB when targeting a BER of 10^{-9}, which is the commonly required performance for fiber optic systems.

B. Receiver Modification

It is also possible to achieve a better BER performance by rotating the decision boundaries according to the asymmetric signal constellation. In Table II, the new boundary angles for the four quadrants are listed for different cutoff frequencies. Those boundary angles are calculated numerically from the theoretical BER analysis by minimizing $(P_1 + P_2)/2$.

The new boundaries applied to the simulated signal

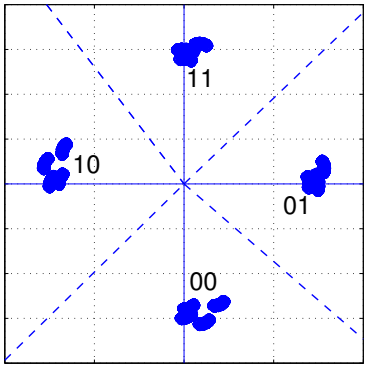

Fig. 17. New decision boundaries for the simulated signal constellation at a cutoff frequency $f_c = 7$ GHz and $E_b/N_0 = 11$ dB.

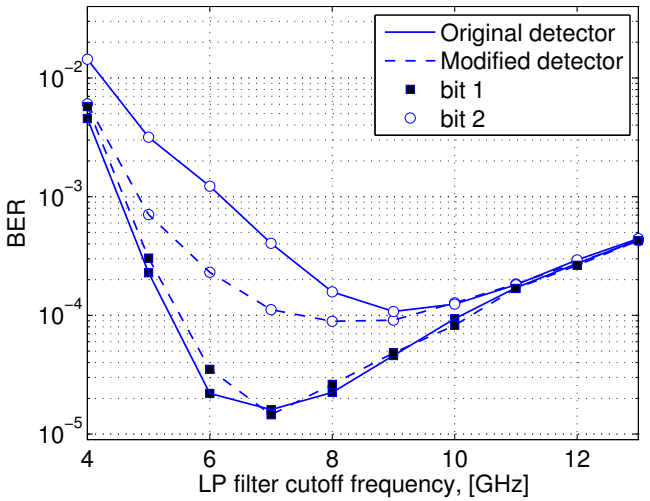

Fig. 18. Performance comparison for systems with and without modified receiver at $E_b/N_0 = 11$ dB.

constellation are shown in Fig. 17. The simulated BER performance versus cutoff frequency for the system with the modified receiver is compared with the old system in Fig. 18. By comparing the mean BER performance for the system with receiver modification to the old system at a fixed cutoff frequency of 7 GHz shown in Fig. 19, we see a similar improvement as the system using the modified transmitter. At very low target BER's, when the performance is entirely determined by the minimum distance, we expect that the transmitter modification will perform better than the receiver modification. It should be noted that the receiver modification can be further improved if the exact Voronoi diagram of the received constellation is calculated and implemented. The improvement is expected to be marginal, but the receiver will be much more complex, since the decision boundaries will not be straight lines and will not meet at the origin.

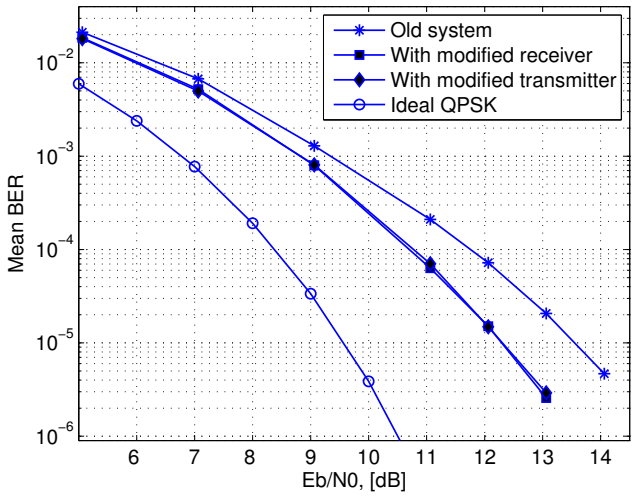

Fig. 19. Performance comparison for systems with and without system modifications at $f_c = 7$ GHz.

VII. Discussion and Conclusions

The use of coherent modulation forms in fiber-optic systems is currently receiving increasing research attention. Fiber-optic QPSK systems are not yet commercially available, but systems and key components are currently being developed [32]–[34] and are likely to reach the market in a few years. Several transmitters of varying complexity and performance have been proposed; in particular, the low-complexity transmitter called transmitter B (TX-B) in this paper is known to carry up to a 2 dB performance penalty compared to more complex transmitters for a DQPSK system [16].

In this paper, we presented and analyzed a unique, novel property of coherent fiber-optic systems with Gray mapped QPSK modulation; namely, that the BER may differ significantly between the bits in a multilevel phase-modulated system. This phenomenon originates in the combined ISI of the electro-optic modulator used in the transmitter and the low-pass filtering used in the receiver. Although the phenomenon itself is not hard to explain, we have not seen it reported previously, and the magnitude of the problem was not anticipated. For the particular systems we investigated, we found that it is most significant in systems based on a single electro-optic phase modulator (TX-B), but it is also clearly present in a transmitter based on one Mach-Zehnder amplitude modulator and one phase modulator (transmitter A, TX-A). The BER difference can exceed ten times already at an average BER of 10^{-4}, and it increases with the SNR.

It should be noted that the unequal BER effect is not significant when the transmitted intensity reaches

zero between the symbols (often called RZ-QPSK) or if a parallel Mach-Zehnder modulator is used [23], [33]. However, these transmitters have a higher complexity, and the RZ-QPSK format requires a higher bandwidth. This BER effect is also not visible in differentially modulated systems.

We found by numerical simulations (and after optimizing the receiver filter bandwidths) that TX-A and TX-B have 1.5 and 4 dB penalty targeting at a BER of 10^{-5}, resp., compared with the ideal Gaussian QPSK channel with maximum likelihood detection. We also found an optimal LP filter bandwidth of around 0.7 times the symbol rate in a coherent QPSK fiber optic system with NRZ pulse format. These findings could be reproduced analytically with reasonable accuracy.

We then considered compensating for the unequal bit error rates by adjusting the transmitted phases. This modification, which mathematically means replacing the standard expression (2) with (12), improved the performance of TX-B by more than 1 dB at a BER of 10^{-5} and is expected to provide about 2 dB gain at 10^{-9}. An alternative compensation technique, based on rotating the receiver decision boundaries, was also studied and turned out to provide a similar improvement. Both compensation methods are relatively simple to implement in the communication hardware at a low, or zero, additional cost. The found improvements can probably be increased further by using more sophisticated methods, such as combining the transmitter and receiver compensation techniques or further optimizing the decision boundaries in the receiver. Equalization techniques, although expensive to implement at these high symbol rates, would undoubtedly reduce the ISI problems further.

In conclusion, the performance loss by using TX-B, which is the most attractive transmitter from a complexity point of view, appears to be less than what has been hitherto believed, provided that some simple compensation technique is applied. On a more general note, the results also emphasize the importance of considering not only the constellation diagram of the system, but also the paths between the symbols, to properly account for the ISI. We thus hope that these findings will be valuable when designing the optical transmitters and receivers in next generation's optical, multilevel coherent systems.

REFERENCES

[1] G. P. Agrawal, *Fiber-Optic Communication Systems*, New York, USA: John Wiley & Sons, Inc., 2002.

[2] J. M. Kahn and K.-P. Ho, "Spectral efficiency limits and modulation/detection techniques for DWDM systems," *IEEE J. Sel. Topics in Quantum Electron.*, vol. 10, no. 2, pp. 259–272, Mar.–Apr. 2004.

[3] J. M. Kahn, "Modulation and detection techniques for optical communication systems," in *Proc. OSA Coherent Optical Technologies and Applications (COTA)*, Whistler, British Columbia, Canada, June 2006.

[4] I. Morita and N. Yoshikane, "Merits of DQPSK for ultrahigh capacity transmission," in *The 18th Annual Meeting of IEEE Lasers and Electro-Optics Society*, Oct. 2005, pp. 487–488.

[5] S. Ferber, C. Schubert, R. Ludwig, C. Boerner, C. Schmidt-Langhorst, and H. G. Weber, "640 Gbit/s DQPSK, single wavelength channel transmission over 480 km fibre link," *Electron. Lett.*, vol. 41, no. 22, pp. 1236–1237, Oct. 2005.

[6] N. Yoshikane and I. Morita, "1.14 b/s/Hz spectrally efficient 50 x 85.4-Gb/s transmission over 300 km using copolarized RZ-DQPSK signals," *IEEE J. Lightwave Tech.*, vol. 23, no. 1, pp. 108–114, Jan. 2005.

[7] L. Christen and A. E. Willner, "System sensitivity of multi-level 16-QAM and QPSK to transmitter imperfections in different modulator designs," in *Proc. OSA Coherent Optical Technologies and Applications (COTA)*, Whistler, British Columbia, Canada, June 2006.

[8] J. G. Proakis, *Digital Communications*, New York: McGraw Hill, 4 ed., 2001.

[9] R. Dogliotti, A. Luvison, and G. Pirani, "Error probability in optical fiber transmission systems," *IEEE Trans. Inform. Theory*, vol. 25, no. 2, pp. 170–178, Mar. 1979.

[10] M. S. Nakhla, "Performance evaluation of optical fiber transmission systems," *IEEE J. Select. Areas Commun.*, vol. 8, no. 8, pp. 1617–1623, Oct. 1990.

[11] P. A. Humblet and M. Azizoğlu, "On the bit error rate of lightwave systems with optical amplifiers," *IEEE J. Lightwave Tech.*, vol. 9, no. 11, pp. 1576–1582, Nov. 1991.

[12] F. Derr, "System performance of an optical QPSK homodyne transmission system with costas loop," *Electron. Lett.*, vol. 14, no. 2, pp. 42–44, 1993.

[13] F. Derr, "Coherent optical QPSK intradyne system: Concept and digital receiver realization," *IEEE J. Lightwave Tech.*, vol. 10, no. 9, pp. 1290–1296, Sept. 1992.

[14] F. Derr, "Optical QPSK homodyne transmission of 280 Mbit/s," *J. of Optical Communications*, vol. 41, no. 22, pp. 401–403, Mar. 1990.

[15] S. Norimatsu, K. Iwashita, and K. Noguchi, "An 8 Gb/s QPSK optical homodyne detection experiment using external-cavity laser diodes," *IEEE Photon. Technol. Lett.*, vol. 4, no. 7, pp. 765–767, Jul. 1992.

[16] M. Ohm and T. Freckmann, "Comparison of different DQPSK transmitters with NRZ and RZ impulse shaping," in *IEEE/LEOS Workshop on Advanced Modulation Formats*, San Francisco, USA, July 2004.

[17] M. Serbay, C. Wree, and W. Rosenkranz, "Comparison of six different RZ-DQPSK transmitter set-ups regarding their tolerance towards fibre impairments in 8x40Gb/s WDM-systems," in *IEEE/LEOS Workshop on Advanced Modulation Formats*, San Francisco, USA, July 2004, pp. 9–10.

[18] M. Pfennigbauer, M. M. Strasser, M. Pauer, and P. J. Winzer, "Dependence of optically preamplified receiver sensitivity on optical and electrical filter bandwidths–measurement and simulation," *IEEE Photon. Technol. Lett.*, vol. 14, no. 6, pp. 831–833, June 2002.

[19] J. S. Lee, Y. C. Chung, and D. J. Digiovanni, "Spectrum-sliced fiber amplifier light source for multichannel WDM applications," *IEEE Photon. Technol. Lett.*, vol. 5, no. 12, pp. 1458–1461, Dec. 1993.

[20] P. J. Winzer, S. Chandrasekhar, and H. Kim, "Impact of filtering on RZ-DPSK reception," *IEEE Photon. Technol. Lett.*, vol. 15, no. 6, pp. 840–842, June 2003.

[21] K.-P. Ho and H.-W. Cuei, "Generation of arbitrary quadrature signals using one dual-drive modulator," *IEEE J. Lightwave Tech.*, vol. 23, no. 2, pp. 764–770, Feb. 2005.

[22] W.-R. Peng, S.-Y. Tsai, J. Chen, and S. Chi, "Comparing the performance of optical DQPSK signal generated by single modulator with and without pulse carver," in *Proc. OSA Coherent Optical Technologies and Applications (COTA)*, Whistler, British Columbia, Canada, June 2006.

[23] H. Zhao, M. Karlsson, and E. Agrell, "Transmitter comparison and unequal bit error probabilities in coherent QPSK systems," in *Proc. Optical Fiber Communication Conference and the National Fiber Optic Engineers Conference, OFC/NFOEC 2007*, Anaheim, USA, Mar. 2007.

[24] F. Forghieri, P. R. Prucnal, R. W. Tkach, and A. R. Chraplyvy, "RZ versus NRZ in nonlinear WDM systems," *IEEE Photon. Technol. Lett.*, vol. 9, no. 7, pp. 1035–1037, July 1997.

[25] M. I. Hayee and A. E. Willner, "NRZ versus RZ in 10–40 Gb/s dispersion-managed WDM transmission systems," *IEEE Photon. Technol. Lett.*, vol. 11, no. 8, pp. 991–993, Aug. 1999.

[26] K.-P. Ho, "Generation of arbitrary quadrature-amplitude modulated signals using a single dual-drive modulator," in *IEEE/LEOS Workshop on Advanced Modulation Formats*, San Francisco, USA, July 2004.

[27] B. E. A. Saleh and M. C. Teich, *Fundamentals of Photonics*, New York, USA: John Wiley & Sons, Inc., 1991.

[28] D. Ly-gagnon, S. Tsukamoto, K. Katoh, and K. Kikuchi, "Coherent detection of optical quadrature phase-shift keying signals with carrier phase estimation," *IEEE J. Lightwave Tech.*, vol. 24, no. 1, pp. 12–21, Jan. 2006.

[29] P. J. Winzer, M. Pfennigbauer, M. M. Strasser, and W. R. Leeb, "Optimum filter bandwidths for optically preamplified NRZ receivers," *IEEE J. Lightwave Tech.*, vol. 19, no. 9, pp. 1263–1273, Sept. 2001.

[30] C. Wang and J. Yan, "*Filter design for noncoherent receivers*," Master Thesis EX023/2006, Department of Signals and Systems, Chalmers University of Technology, Göteborg, Sweden, 2006.

[31] J. D. Downie, I. Tomkos, N. Antoniades, and A. Boskovic, "Effects of filter concatenation for directly modulated transmission lasers at 2.5 and 10 Gb/s," *IEEE J. Lightwave Tech.*, vol. 20, no. 2, pp. 218–228, Feb. 2002.

[32] I. Shpantzer, "Fieldable digital coherent interferometric communication and sensing application domains," in *Proc. OSA Coherent Optical Technologies and Applications (COTA)*, Whistler, British Columbia, Canada, June 2006.

[33] T. Kawanishi, T. Sakamoto, T. Miyazaki, and M. Izutsu, "Integrated $\mathrm{LiNbO_3}$ modulator for high-speed optical quadrature phase shift keying," in *Proc. OSA Coherent Optical Technologies and Applications (COTA)*, Whistler, British Columbia, Canada, June 2006.

[34] P. S. Cho, G. Harston, A. Greenblatt, A. Kaplan, Y. Achiam, R. M. Bertenburg, A. Brennemann, B. Adoram, P. Goldgeier, and A. Hershkovits, "Integrated optical coherent balanced receiver," in *Proc. OSA Coherent Optical Technologies and Applications (COTA)*, Whistler, British Columbia, Canada, June 2006.